DALTON
FULL PAPER

^{1}H NMR study of 2-methylimidazole binding to cytochrome c: a comprehensive investigation of the role of the methyl substituent on the ligand binding affinity and heme electronic structure in imidazole–cytochrome c complexes

Yong Yao, Chengmin Qian, Yibing Wu, Jun Hu and Wenxia Tang*

Coordination Chemistry Institute, State Key Laboratory of Coordination Chemistry, Nanjing University, Nanjing 210093, P. R. China. E-mail: wxtang@netra.nju.edu.cn

Received 3rd January 2001, Accepted 17th April 2001
First published as an Advance Article on the web 22nd May 2001

The binding of 2-methylimidazole (2mim) to horse heart cytochrome c (hh cyt c) has been studied by NMR spectroscopy. Some proton resonances were assigned and the kinetic and thermodynamic parameters for the binding were presented. Based on its unique hyperfine shift pattern and the anomalous temperature dependence of the heme methyl resonances, the heme electronic structure was discussed and the orientation of the bound 2mim was estimated. With these data, a comprehensive comparison of imidazole (Him), 4-methylimidazole (4mim) and 2mim bound cyt c complexes was made on the ligand binding affinity and the heme electronic structure. Different properties in these ligand–cyt c complexes provide a useful lesson for the study of protein–small molecular interactions.

Introduction

Mitochondrial cytochrome c (cyt c) is one of the most well-characterized proteins because of its important physiological role as an electron carrier in various biological redox processes. Extensive studies have been performed on this metalloprotein with the aim of obtaining the correlation of the protein structure with its function.[1–4] It has been shown by optical and NMR spectroscopy that the distal axial ligand in oxidized cyt c, Met80, dissociates more readily and can be displaced by exogenous ligands.[5,6] The ligand–cyt c complex is an excellent model for analogy to the cyt c folding intermediate. Until now, efforts have been focused on the interaction between cyt c and various exogenous ligands such as CN^-, imidazole, pyridine and NH_3.[5–11]

The electron transfer mechanism of cyt c is ultimately linked to the electronic structure and magnetic properties of the heme. Generally speaking, the protein environment introduces a rhombic perturbation at some arbitrary angle θ with respect to the iron-centered reference coordinate system and therefore resolves the degeneracy of the ground state of heme iron.[12] The rhombic perturbation θ and the energy splitting parameter ΔE determine the electronic structure of the heme moiety and result in the heme hyper-fine shift patterns and their temperature dependence.[12–17] In ferric cyt c, it has been proposed that the orientation of the histidine and methionine axial ligands dominates the rhombic perturbation and that the two ligands have approximately equal influence.[13] The pairwise pattern of the heme methyl hyper-fine shifts and their 'anomalous' temperature dependence for cyt c have been interpreted successfully based on the above theoretical analysis.[16]

Ligand bound cyt c is also a model for the heme electronic structure study because the nature and geometry of different ligands results in various heme electronic structures.[6,11,17] As analogous complexes of bis-histidinyl heme c proteins, imidazole (Him) and 4-methylimidazole (4mim) bound cyt c have been studied by NMR spectroscopy.[8,10,11] It was shown that the introduction of a methyl substituent in 4mim–cyt c noticeably alters the orientation of the bound exogenous ligand and heme electronic structure compared to Him–cyt c.[11] Bearing in mind that 2-methylimidazole (2mim) has a significant hindrance effect and that it stabilizes a rare electronic ground state in some model complexes,[18,19] we report herein, our investigations into 2mim binding to cyt c and make a comprehensive comparison of imidazole and its methyl derivatives bound to cytochrome c complexes on the ligand binding affinity and electronic structure of the heme by NMR spectroscopy in order to gain a deeper insight into the interaction between small ligands and cyt c.

Experimental

Sample preparation

Horse heart cyt c (type VI) was purchased from Sigma Chemical Co. and purified as previously described.[20] 2mim was bought from ACROS ORGANICS and used without purification. The NMR samples consisted of 6 mM cyt c and 1 M 2mim in D_2O in which the ratio of native cyt c to 2mim–cyt c is about 1 : 1. The pH of the samples was adjusted to 7.0 by addition of small volumes of DCl. The pH readings were uncorrected for the isotope effect.

NMR spectroscopy

All the ^{1}H NMR experiments were performed on a Bruker AM 500 spectrometer equipped with an Aspect 3000 computer system. Typically, 16k data points over a sweep width of 35.7 kHz were obtained for one-dimensional spectra. For two-dimensional spectra, 512 × 2048 time domain data with a sweep width of 35.7 kHz in F_2 dimension were used, applying 128 scans for each t_1 increment. The carrier was centered on the residual water peak which was suppressed by presaturation during the relaxation delay. Chemical shift values are referenced to 1,4-dioxane at 3.74 ppm.

The detection of 2-D EXSY spectra was achieved using the standard NOESY pulse sequence with a mixing time of 25 ms. Raw data were multiplied in both dimensions by a shifted sine-

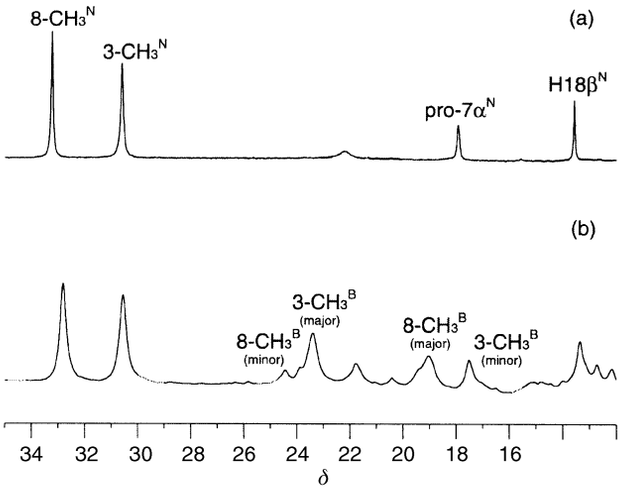

Fig. 1 Downfield hyperfine-shifted region of the ^{1}H NMR spectra in D_2O at 313 K, pH 7.0 of (a) native cyt c only and (b) cyt c with 1 M 2mim. Resonances due to cyt c and 2mim–cyt c are labelled with N and B respectively.

squared window function and Fourier transformed to obtain 1k × 1k real data points. A polynomial base-line correction was applied in both directions. Data processing was performed using the standard Bruker software package XWINNMR (version 2.6, Bruker Analytik GmbH, Rheinstetten, Germany, 1999).

The integral values of the two-dimensional peaks were obtained by direct reading from the spectra using a square frame, and normalized according to $\Sigma I_{ij} = 1$. The same frame was used to estimate the average noise integral value in order to remove the noise effect from the quantitative two-dimensional integration, and I_{ij} were corrected before normalization. The equilibrium magnetization values were obtained by integration in the one-dimensional spectra and also normalized.

Results and discussion

Binding affinity to cyt c

The downfield hyperfine shifted portions of the ^{1}H NMR spectra of native cyt c and of mixtures containing cyt c and 2mim–cyt c are presented in Fig. 1. It is obvious that the presence of 2mim causes the appearance of new resonances in the hyperfine shifted region which indicates the formation of 2mim–cyt c. In the downfield region of the 2-D EXSY spectrum (Fig. 2), a signal at 32.83 ppm which is known as the heme 8-CH_3 resonance of cyt c is connected to a strong cross peak at 18.98 ppm and a weak one at 24.41 ppm. The two signals are assigned to 8-CH_3 of 2mim–cyt c, suggesting that the ligation of 2mim to cyt c causes the formation of two components, which we refer to as the major and minor form. An EXSY cross peak is detected between 8-CH_3 of the two forms, indicating that the two interconvertible components of 2mim–cyt c exchange at a rate slow enough to be observed on the NMR timescale. The kinetic process of 2mim binding to cyt c can be represented by eqn. (1):

$$\begin{aligned} &\text{cyt c} + 2\text{mim} \underset{k_{21}}{\overset{k_{12}}{\rightleftharpoons}} \text{2mim-cyt c (I, minor)}\ K_1 \\ &\text{cyt c} + 2\text{mim} \underset{k_{31}}{\overset{k_{13}}{\rightleftharpoons}} \text{2mim-cyt c (II, minor)}\ K_2 \\ &\text{2mim-cyt c} \underset{k_{32}}{\overset{k_{23}}{\rightleftharpoons}} \text{2mim-cyt c (II)}\ K_3 \end{aligned} \quad (1)$$

In the case of the reactions in eqn. (1), the magnetization exchange between these species follows a first-order rate process eqn. (2):

The relationship between the magnetization exchange rate constants and the exchange rate constants can be found in

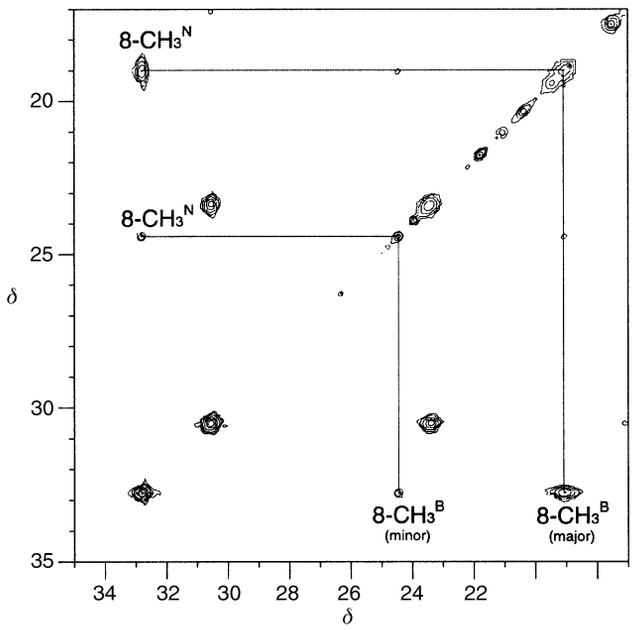

Fig. 2 Portions of the EXSY spectrum of cyt c with 1 M 2mim at pH 7.0 and 313 K, mixing time 25 ms, indicating the formation of two components of 2mim–cyt c. Labelling as in Fig. 1.

$$\begin{aligned} M_{\text{cyt c}} &\underset{k_{BA}}{\overset{k_{AB}}{\rightleftharpoons}} M_{\text{2mim-cyt c (I)}} \\ M_{\text{cyt c}} &\underset{k_{CA}}{\overset{k_{AC}}{\rightleftharpoons}} M_{\text{2mim-cyt c (II)}} \\ M_{\text{2mim-cyt c (I)}} &\underset{k_{CB}}{\overset{k_{BC}}{\rightleftharpoons}} M_{\text{2mim-cyt c (II)}} \end{aligned} \quad (2)$$

eqn. (3), and the apparent equilibrium constant K_{app} and the equilibrium constant K of these reactions can be calculated from eqns. (4) and (5) where k_a is the dissociation constant of 2mim.

$$\begin{aligned} k_{12} = k_{AB}/[2\text{mim}],\ k_{21} = k_{BA} \\ k_{13} = k_{AC}/[2\text{mim}],\ k_{31} = k_{CA} \\ k_{23} = k_{BC},\ k_{32} = k_{CB} \end{aligned} \quad (3)$$

$$\begin{aligned} K_{app1} &= k_{12}/k_{21} \\ K_{app2} &= k_{13}/k_{31} \\ K_{app3} &= k_{23}/k_{32} \end{aligned} \quad (4)$$

$$\begin{aligned} K_1 &= K_{app1}\ (1 + [H^+]/k_a) \\ K_2 &= K_{app2}\ (1 + [H^+]/k_a) \\ K_3 &= K_{app3} \end{aligned} \quad (5)$$

According to the theory of ligand binding kinetics studied by exchange spectroscopy,[21,22] the reaction amplitude matrix A based on the integration of 8-CH_3 at 315 K and pH 7.0 is obtained as:

$$A = \begin{bmatrix} 0.521 & 0.372 & 0.430 \\ 0.058 & 0.499 & 0.079 \\ 0.285 & 0.320 & 0.484 \end{bmatrix} \quad (6)$$

the kinetic matrix R is calculated to be:

$$R = \begin{bmatrix} 39.8 & -21.8 & -41.1 \\ 3.31 & 30.6 & -5.44 \\ -27.4 & -21.5 & 44.0 \end{bmatrix} \quad (7)$$

Thus the magnetization exchange rate constants are: $k_{AB} = 3.31\ s^{-1}$, $k_{BA} = 21.8\ s^{-1}$, $k_{AC} = 27.4\ s^{-1}$, $k_{CA} = 41.1\ s^{-1}$,

Table 1 Rate and equilibrium constants for binding of 2mim to cyt c at different temperatures

T/K	k_1/dm^3 mol^{-1} s^{-1}	k_{-1}/s^{-1}	K_{app}/dm^3 mol^{-1}	K/dm^3 mol^{-1}
313	23.0	43.4	0.529	4.27
315	27.1	41.1	0.667	5.39
318	35.5	42.0	0.864	6.98
320	40.3	39.5	1.02	8.24

Table 2 Thermodynamic parameters of reactions of cyt c with Him, 4mim and 2mim

Reaction	K(315 K)/ dm^3 mol^{-1}	$\Delta H°$/ kJ mol^{-1}	$\Delta S°$/ J mol^{-1} K^{-1}
Him and cyt c [a]	37.8	56.8	210
4mim and cyt c [a]	38.4	135	459
2mim and cyt c	5.39	77.4	259

[a] Calculated from the data of ref. 11.

$k_{BC} = 21.5$ s^{-1} and $k_{CB} = 5.44$ s^{-1}. The reaction rate constants are calculated to be: $k_{12} = 3.31$ M^{-1} s^{-1}, $k_{21} = 21.8$ s^{-1}, $k_{13} = 27.4$ M^{-1} s^{-1}, $k_{31} = 41.1$ s^{-1}, $k_{23} = 21.5$ s^{-1} and $k_{32} = 5.44$ s^{-1}. Then the equilibrium constants are: $K_{app1} = 0.152$ M^{-1}, $K_{app2} = 0.667$ M^{-1}, $K_{app3} = 3.97$, $K_1 = 1.23$ M^{-1}, $K_2 = 5.39$ M^{-1} and $K_3 = 3.97$. The major species has an association rate and dissociation rate much faster than the minor one (8 times and 2 times respectively), and the ratio of their association constants is about 4. Such a difference is attributed to two orientations of 2mim binding to cyt c, relating to the differences in the steric accessibility to the heme. Obviously, the formation of the minor form of 2mim–cyt c is more sterically hindered than the major one.

The kinetic and equilibrium data for the binding of 2mim to cyt c (because of the small fraction of the minor form, only the major form is considered and referred to as 2mim–cyt c unless otherwise stated) were obtained at different temperatures and are given in Table 1. The $\Delta H°$ and $\Delta S°$ values for the complexation were obtained by least-squares fitting from Table 1 according to the van't Hoff equations and are listed in Table 2. From Table 2 it follows that at 315 K the affinity of Him and its methyl derivatives to cyt c have the order: 4mim ≈ Him >> 2mim. The association constant of 4mim–cyt c is almost the same as Him–cyt c. However, the temperature dependence of the association constant for 4mim–cyt c is much larger than that for Him–cyt c and this can be interpreted as a consequence of a larger entropy increase upon ligation.[11] The association constant of 2mim–cyt c at 315 K is only 14% of that of 4mim–cyt c and Him–cyt c. Such a low affinity is dominated by the prevention of the approach of 2mim to the heme imposed by the steric hindrance between the methyl group and the heme ring.

As seen from Table 2, the $\Delta H°$ and $\Delta S°$ for the binding of Him, 4mim and 2mim to cyt c are both positive. Cyt c was thought to provide a hydrophobic environment for the heme.[23] A hydrophobic environment is equivalent to a medium of low dielectric constant, which results in a negative $\Delta H°$. On the other hand, Him and its derivatives are bulky ligands and are sterically hindered from entering the heme pocket. The steric effect upon ligation will contribute to a positive $\Delta H°$. These factors interplay, and the apparent $\Delta H°$ measured reflects their net effect. It can be calculated that when $T = 303$ K or above, all reactions have negative Δ. This suggests that all these reactions are driven by a favorable entropy change. It is noted that the values of $\Delta H°$ and $\Delta S°$ of these reactions have the following order: 4mim > 2mim > Him. To give a rational interpretation in structural terms, the structure of 4mim–cyt c and 2mim–cyt c (Fig. 3) were proposed through molecular modeling using the Sander module of the AMBER package.[24] A template coordinate set was generated by adding a methyl to the Him moiety

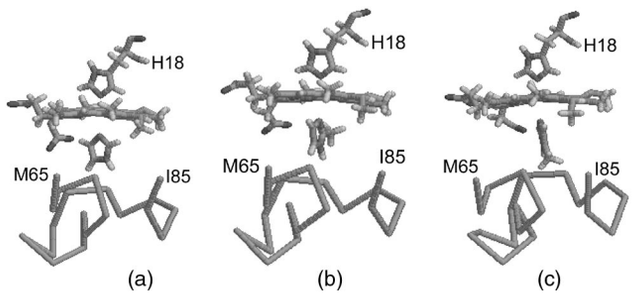

Fig. 3 Structures of the heme cavity in Him–cyt c (PDB entry 1FI9) (a), 4mim–cyt c (b) and 2mim–cyt c (c).

based on the solution structure of Him–cyt c (PDB entry 1FI9).[10] The starting template underwent 6000 steps REM to give the final structure. Restraints from NOEs[11] and interpretations of the hyperfine pattern were introduced during the energy minimization to determine the orientations of imidazole in 2mim–cyt c and 4mim–cyt c. Comparing these three structures shows that the overall fold of the protein is almost the same and the difference is focused on the local conformation of peptides near the heme cavity and the orientation of the exogenous ligand (Fig. 3). Him binding to cyt c causes significant perturbation to the conformation of cyt c in peptides 75–85.[10] These residues rearrange to accommodate the exogenous Him and the orientation of the imidazole is almost parallel to His18. As for the binding of 2mim to cyt c, the substituent prevents 2mim approaching to the heme. However, inspection of the structure of 2mim–cyt c showed that 2mim did not cause a noticeable deformation of the heme ring and it adopted an orientation whereby the methyl pointed towards the open crevice of the heme hydrophobic cavity so as to minimize its steric hindrance. Compared to Him–cyt c, there is no obvious structural difference except for the displacement of some hydrophobic residues (Ile81 as an example) near the methyl of 2mim. Thus, binding of 2mim to cyt c causes a slightly larger $\Delta H°$ and $\Delta S°$ than Him. In 4mim–cyt c, the differently orientated methyl substituent points towards the residues which constitute the heme hydrophobic pocket. The resulting repulsions between the methyl group and the surrounding residues cause the most significant conformational change of the peptides from Met65 to Ile85 and results in the largest enthalpy and entropy increase.

Hyperfine shift pattern and the heme electronic structure

As most of the resonances of cyt c have been assigned,[4,25] the 2-D EXSY method can be used to determine the corresponding resonance assignments of 2mim–cyt c (Fig. 4). The assignments of the heme peripheral protons and some protons of the residues near the heme pocket are summarized in Table 3.

In low-spin ferriheme proteins, rhombic perturbation θ approximately equals the angle between the bisector of the projections of the two axial ligands and the Fe–NB direction.[10,12] The average nodal plane of these ligands determines the molecular x and y direction by giving rise to linear combinations of the porphyrin π orbitals and metal d_π orbitals of the type:

$$\phi_x = \cos\theta(|d_{xz}> + |\pi_x>) + \sin\theta(|d_{yz}> + |\pi_y>) \quad (8a)$$

$$\phi_y = \cos\theta(|d_{yz}> + |\pi_y>) - \sin\theta(|d_{xz}> + |\pi_x>) \quad (8b)$$

When $\theta = 0°$ (or 90° depending on whether the ground state is φ_y or φ_x), spin density is delocalized primarily into pyrroles A and C in the ground state. For an alignment along the meso–Fe–meso vector (*i.e.* $\theta = 45°$), the equal participation of π_x and π_y in eqn. (8) results in comparable spin density in each pyrrole. In native cyt c, the average orientation of the axial ligands is 71°

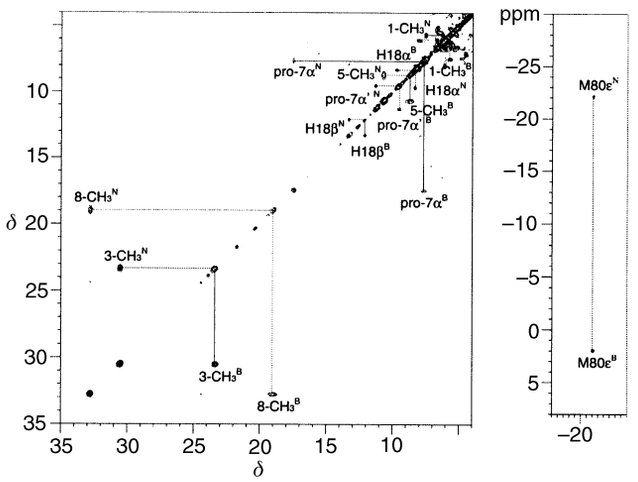

Fig. 4 Downfield and upfield regions of the EXSY spectrum of cyt c with 1 M 2mim at pH 7.0 and 313 K, mixing time 25 ms. Labelling as in Fig. 1.

Table 3 Shift values of the hyperfine shifted signals of 2mim–cyt c (pH = 7.0, T = 313 K)

Assignment	δ
3-CH_3	23.45
8-CH_3	18.98
5-CH_3	8.69
1-CH_3	5.68
7-Hα	9.55
7-Hα'	7.65
Thioether-2	−0.92
His18-α	9.70
His18-β	12.14
His18-β'	8.33
Leu68-δ_1	−0.50
Leu68-δ_2	−1.76
Pro71-α	5.80
Thr78-α	6.70
Thr78-β	6.43
Phe82(*o*)	8.19
Phe82(*m*)	6.81
Phe82(*p*)	6.69
Met80-ε	1.99

and θ was calculated to be 85° by fitting ^{13}C contact shifts.[14] Because the MO is close, although not exactly aligned to the direction defined by the pyrrole nitrogen atoms (Fig. 5), the electron spin is primarily located in pyrroles B and D, and results in large contact shifts for 8-CH_3 and 3-CH_3, which contributes to a pairwise pattern of the heme methyl shifts on opposite pyrrole rings (Table 4).

For Him–cyt c and 4mim–cyt c, the axial ligands impart the rhombic perturbation $\theta = 45°$ and 60° respectively.[10,11] The corresponding MOs lie approximately near the α/γ direction, which cause the disappearance of the pairwise pattern. The chemical shifts of 8-CH_3 and 3-CH_3 move upfield, while 5-CH_3 and 1-CH_3 move downfield. The heme methyl resonances of Him–cyt c and 4mim–cyt c thus have a much smaller spread compared to hh cyt c (Table 4), indicating that these complexes have higher symmetry for the electron spin distribution relative to hh cyt c. However, there is still some difference in the hyperfine shift pattern of Him–cyt c and 4mim–cyt c. The smallest spin density is found for 1-CH_3 in Him–cyt c, while in the latter it is found in 5-CH_3.

As in 2mim–cyt c, unlike other ligand–cyt c complexes,[6,9,11] the ligation of 2mim to the heme iron does not cause the disappearance of the pairwise pattern of the heme methyl shifts. All four methyl shifts move upfield compared to cyt c and have the order: 3-CH_3 > 8-CH_3 >> 5-CH_3 > 1-CH_3 (Table 4). This order resembles that of a bis-histidine coordination hemoprotein *M. methylotrophus* cyt c which is believed to have the two histidine ligands in nearly perpendicular relative orientations.[26] The latter has the observed methyl shifts (3-CH_3 > 8-CH_3 > 5-CH_3 > 1-CH_3): 18.1, 15.1, 12.9 and 8.4 ppm, with the axial imidazole plane angles *ca.* 75° and 155°, supplying θ about 115°.[25] It is believed that the heme methyl shift order has an intimate relation to the orientation of the axial ligands. According to the studies of Shokhirev and Walker,[27] such a methyl shift order suggests a θ value between 95° and 125°. Based on the characteristic pairwise hyperfine shift pattern, it is reasonable to estimate the rhombic perturbation θ in 2mim–cyt c to be about 90°. If we suppose His-18 and 2mim contribute equally to the rhombic perturbation and that His-18 retains its orientation upon ligation, the orientation of 2mim should be near to the β/δ direction. Using this as a constraint, a structure of 2mim–cyt c was obtained by molecular modeling. Results show that the two imidazole planes have perpendicular orientations in 2mim–cyt c (Fig. 3).

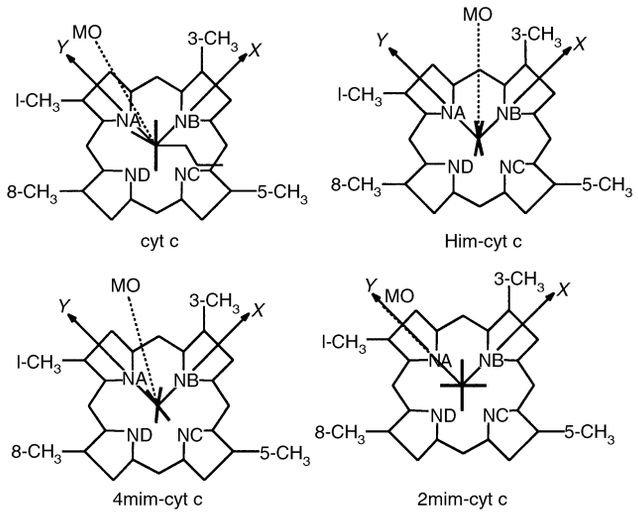

Fig. 5 Illustration of ligand orientations and the rhombic perturbation (labelled MO) in cyt c, Him–cyt c, 4mim–cyt c and 2mim–cyt c.

The orientations of the axial ligands and the rhombic perturbation angles in cyt c, Him–cyt c, 4mim–cyt c and 2mim–cyt c are illustrated in Fig. 5. It shows that the orientation of His18 remains unchanged in cyt c and ligand–cyt c complexes, which is coincident with the ideal that ligand binding to cyt c only causes local conformational changes and that the overall fold of the protein is unaffected, while the other ligand orientation can differ noticeably. In native hh cyt c, Met80 adopts an orientation such that the π MO with the electron spin encompasses the most exposed heme edge.[11] Associating that heme edge with the cytochrome's redox interface contributes to the proposal that the electronic structure, proton hyperfine resonance pattern and electron-transfer properties were defined by the Met chirality. In ligand–cyt c complexes, it is the ligand geometry that determines the interaction between the ligand and the surrounding protein matrix, and then the exogenous ligand orientation. In bis-imidazole heme complexes, molecular mechanics calculations have predicted that the parallel conformation is more stable than the perpendicular one.[28] This is true in the Him–cyt c complex, but fails for the 4mim–cyt c and 2mim–cyt c complexes. The steric interaction between the methyl substituent and the protein matrix constrains the 'free rotation' around the Fe–Nε axis and only certain orientations are preferable. Such a hindrance effect causes the two imidazole planes to form an angle of 46° in 4mim–cyt c[11] and a perpendicular conformation in 2mim–cyt c. The different orientations of the exogenous ligands in these ligand–cyt c complexes predominates their electronic structures, which is reflected in the different heme hyperfine shift patterns obtained.

Table 4 Hyperfine shift pattern, axial ligand orientation and rhombic perturbation parameter of native cyt c, Him–cyt c, 4mim–cyt c and 2mim–cyt c

	Methyl order	Methyl shifts/ppm	Shift spread/ppm	Ligand orientations/°	θ/°
hh cyt c [a]	8 > 3 >> 5 > 1	32.82, 30.56, 10.67, 7.52	25.30	48(H), 93(M)	85
Him–cyt c [b]	8 >3 > 5 > 1	24.94, 17.41, 13.61, 10.25	14.69	41(H), 48(Him)	45
4mim–cyt c [bc]	8 >3 > 1 > 5	25.01, 19.05, 13.24, 11.70	13.31	40(H), 90(4mim)	60
2mim–cyt c [c]	3 >8 >> 5 > 1	23.45, 18.98, 8.69, 5.68	17.77	45(H), 135(2mim)	90

[a] Refs. 13 and 27. [b] Ref. 10. [c] Ligand orientations were calculated from the structure obtained by molecular modeling.

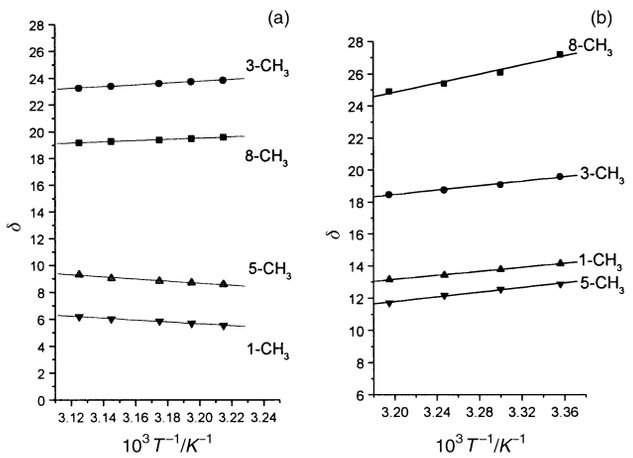

Fig. 6 Temperature dependence of the heme methyl resonances of 2mim–cyt c (a) and 4mim–cyt c (b).

Temperature dependence of heme methyl resonances

The observed temperature dependence can be interpreted in terms of the heme electronic structure on the basis of the reasonable assumption that the contact contribution dominates the heme hyperfine shifts. In a simplistic picture, the MO along the N–Fe–N vectors through pyrroles A and C will have the ground $(d_{xy})^2(d_{yz})^2(d_{xz})^1$ and excited $(d_{xy})^2(d_{xz})^2(d_{yz})^1$ orbital states.[12,16] The ground state will exhibit large B(3-CH_3) and D(8-CH_3) and negligible A(1-CH_3) and C(5-CH_3) pyrrole contact shifts, while the excited states will display large contact shifts for pyrroles A(1-CH_3) and C(5-CH_3), but none for pyrroles B(3-CH_3) and D(8-CH_3). The observed mean $\delta_{hf}(T)$ will obey the equation:

$$\delta_{hf}(T) = [\delta_{hf}{}^{g}(T) + \delta_{hf}{}^{e}(T)e^{-\Delta E/RT}][1 + e^{-\Delta E/RT}]^{-1} \quad (9)$$

with g as ground state, e as excited state and ΔE as the energy spacing. For the case where ΔE is comparable to kT, and we assume strict Curie behavior for δ_{hf} for a single orbital state, raising the temperature to populate the excited state should lead to hyper-Curie behavior for the methyls of pyrroles B and D, and hypo-Curie or even anti-Curie behavior for the methyls of pyrroles A and C. Inspection of Fig 5 reveals that this is qualitatively the behavior shown by 4mim–cyt c and 2mim–cyt c for the heme methyls.

The observed 'anomalous' temperature behavior related to population of the excited state is linked to the magnitude of the orbital spacing which, in turn, can provide information on the axial Fe–ligand bond strength.[12,16,29] Simulations of the predicted temperature dependence based on eqn. (9) shows that anti-Curie behavior can be observed only when the energy spacing is small enough.[30] The different temperature dependence of the heme methyl shifts in 4mim–cyt c and 2mim–cyt c (Fig. 6) indicates that the energy splitting in 4mim–cyt c is larger than that in 2mim–cyt c, which gives us the ideal that the Fe–Nε bond in 2mim–cyt c is weaker than the bond in 4mim–cyt c. This could be validated by the fact that the methyl orientation prevents 2mim approaching the heme and the much smaller association constant of 2mim–cyt c (Table 2).

References

1 G. R. Moore and G. W. Pettigrew, *Cytochrome c, Evolutionary Structural and Phylogical Aspects*, Springer-Verlag, Berlin, 1990.
2 J. R. Winker and H. B. Gray, *Chem. Rev.*, 1992, **92**, 369.
3 P. X. Qi, R. A. Beckman and A. J. Wand, *Biochemistry*, 1996, **35**, 12275.
4 L. Banci, I. Bertini, H. B. Gray, C. Luchinat, T. Reddig, A. Rosato and P. Turano, *Biochemistry*, 1997, **36**, 9867.
5 W. P. Shao, Y. M. Yao, G. H. Liu and W. X. Tang, *Inorg. Chem.*, 1993, **32**, 6112.
6 L. Banci, I. Bertini, G. A. Spyroulias and P. Turano, *Eur. J. Inorg. Chem.*, 1998, 583.
7 W. P. Shao, H. Z. Sun, Y. M. Yao and W. X. Tang, *Inorg. Chem.*, 1995, **34**, 680.
8 G. H. Liu, W. P. Shao, X. L. Huang, H. M. Wu and W. X. Tang, *Biochim. Biophys. Acta*, 1996, **1277**, 61.
9 K. L. Bren, H. B. Gray, L. Banci, I. Bertini and P. Turano, *J. Am. Chem. Soc.*, 1995, **117**, 8067.
10 L. Banci, I. Bertini, G. Liu, J. Lu, T. Reddig, W. Tang, Y. Wu, Y. Yaoand D. Zhu, *J. Biol. Inorg. Chem.*, 2001, in press.
11 Y. Yao, Y. B. Wu, C. M. Qian and W. X. Tang, *J. Chem. Soc., Dalton Trans.*, 2000, **22**, 4069.
12 G. N. La Mar, J. D. Satterlee and J. S. De Ropp, *Nuclear Magnetic Resonance of Hemoproteins*, Academic Press, New York, 2000.
13 D. L. Turner, *Eur. J. Biochem.*, 1995, **227**, 829.
14 L. Banci, R. Pierattelli and D. L. Turner, *Eur. J. Biochem.*, 1995, **232**, 522.
15 N. V. Shokhirev and F. A. Walker, *J. Am. Chem. Soc.*, 1998, **120**, 981.
16 L. Banci, I. Bertini, C. Luchinat, R. Pierattelli, N. V. Shokhirev and F. A. Walker, *J. Am. Chem. Soc.*, 1998, **120**, 8472.
17 L. Brennman and D. L. Turner, *Biochim. Biophys. Acta*, 1997, **1342**, 1.
18 S. Wolowiec, L. Latos-Grazynski, M. Mazzanti and J. Marchon, *Inorg. Chem.*, 1997, **36**, 5761.
19 F. A. Walker and U. Simonis, *Biological Magnetic Resonances Volume 12 NMR of Paramagnetic Molecules*, Plenum Press, New York, 1993.
20 G. Williams, G. R. Moore, R. Porteous, M. N. Robinson, N. Soffe and R. J. P. Williams, *J. Mol. Biol.*, 1985, **183**, 409.
21 R. R. Ernst, G. Bodenhausen and A. Wokaun, *Principles of Nuclear Magnetic Resonances in One and Two Dimensions*, Oxford University Press, London, 1987.
22 E. R. Johnston, M. J. Dellwo and J. Hendrix, *J. Magn. Reson.*, 1986, **66**, 399.
23 M. M. M. Saleem and M. T. Wilson, *Inorg. Chim. Acta*, 1988, **153**, 105.
24 D. A. Pearlman, D. A. Case, J. W. Caldwell, W. S. Ross, T. E. Cheatham, D. M. Ferguson, G. L. Seibel, U. C. Singh, P. K. Weiner and P. A. Kollman, AMBER 5.0, University of California, San Francisco, 1997.
25 Y. Feng, H. Roder, S. W. Englander, A. J. Wang and D. L. Di Stefano, *Biochemistry*, 1989, **28**, 195.
26 H. S. Costa, H. Santos and D. L. Turner, *Eur. J. Biochem.*, 1993, **215**, 817.
27 N. V. Shokhirev and F. A. Walker, *J. Biol. Inorg. Chem.*, 1998, **3**, 581.
28 L. A. Herbert, F. George, P. A. James, J. C. Arthur, W. D. Michael, T. H. Barbara and C. R. Douglas, *Acta Crystallogr., Sect. D*, 1994, **50**, 596.
29 B. D. Nguyen, Z. C. Xia, D. C. Yeh, K. Vyas, H. Deaguero and G. N. Lar Mar, *J. Am. Chem. Soc.*, 1999, **121**, 208.
30 U. Kolczak, J. B. Hauksson, N. L. Davis, U. Pande, J. S. De Ropp, K. C. Langry, K. M. Smith and G. N. Lar Mar, *J. Am. Chem. Soc.*, 1999, **121**, 83.